

## Photocatalysis

Photocatalytic Arylation of P<sub>4</sub> and PH<sub>3</sub>: Reaction Development Through Mechanistic Insight

Robin Rothfelder, Verena Streitferdt, Ulrich Lennert, Jose Cammarata, Daniel J. Scott, Kirsten Zeitler, Ruth M. Gschwind,\* and Robert Wolf\*

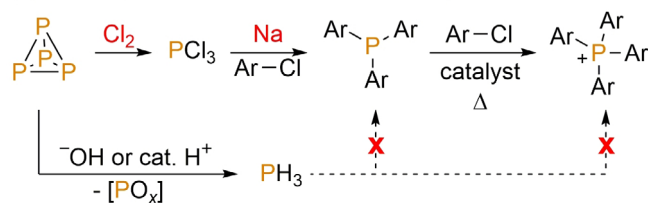
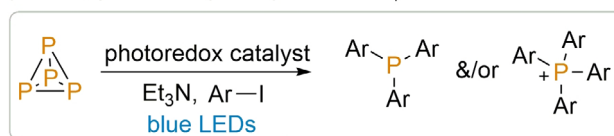
Dedicated to Professor Holger Braunschweig on the occasion of his 60th birthday

**Abstract:** Detailed <sup>31</sup>P{<sup>1</sup>H} NMR spectroscopic investigations provide deeper insight into the complex, multi-step mechanisms involved in the recently reported photocatalytic arylation of white phosphorus (P<sub>4</sub>). Specifically, these studies have identified a number of previously unrecognized side products, which arise from an unexpected non-innocent behavior of the commonly employed terminal reductant Et<sub>3</sub>N. The different rate of formation of these products explains discrepancies in the performance of the two most effective catalysts, [Ir(dtbbpy)(ppy)<sub>2</sub>][PF<sub>6</sub>] (dtbbpy = 4,4'-di-*tert*-butyl-2,2'-bipyridine) and 3DPAFIPN. Inspired by the observation of PH<sub>3</sub> as a minor intermediate, we have developed the first catalytic procedure for the arylation of this key industrial compound. Similar to P<sub>4</sub> arylation, this method affords valuable triarylphosphines or tetraarylphosphonium salts depending on the steric profile of the aryl substituents.

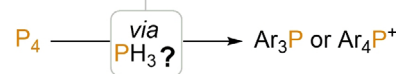
## Introduction

White phosphorus (P<sub>4</sub>) is the common precursor from which all organophosphorus compounds (OPCs) are currently prepared.<sup>[1]</sup> The enormous range of important applications of these compounds (including pharmaceuticals, agrochemicals, photoinitiators, catalysts, *et cetera*) makes P<sub>4</sub> one of the most important single precursors for the modern chemical industry.<sup>[2]</sup> Unfortunately, current methods for the use of

elemental phosphorus suffer from major drawbacks, including difficulties in the initial preparation of P<sub>4</sub> from phosphate minerals as well as problems relating to phosphorus recovery and recycling.<sup>[3]</sup> Particularly significant are serious limitations in state-of-the-art methods for the transformation of P<sub>4</sub> into useful OPCs, which rely on wasteful and inefficient multi-step procedures involving extremely hazardous and difficult-to-handle reagents and intermediates.<sup>[4]</sup> These problems are exemplified in the syntheses of arylated phosphines (Ar<sub>3</sub>P) and phosphonium salts (Ar<sub>4</sub>P<sup>+</sup>), which find important commercial applications in catalysis (among many other areas)

(a) Current, indirect industrial routes to Ar<sub>3</sub>P, Ar<sub>4</sub>P<sup>+</sup>(b) Direct, photocatalytic arylation of P<sub>4</sub>

(c) This work:



Mechanistic understanding → New reactivity

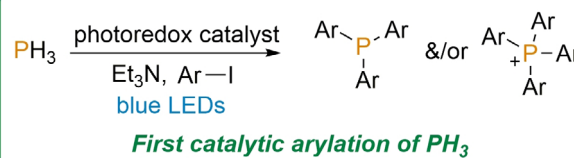


**Figure 1.** a) Indirect, stepwise methods for the synthesis of triarylphosphines Ar<sub>3</sub>P and tetraarylphosphoniums Ar<sub>4</sub>P<sup>+</sup> employed industrially; b) recently reported direct photocatalytic transformation of P<sub>4</sub> into Ar<sub>3</sub>P and Ar<sub>4</sub>P<sup>+</sup> and c) direct photocatalytic arylation of PH<sub>3</sub> described herein, developed based on improved mechanistic understanding of P<sub>4</sub> arylation.<sup>[9]</sup>

[\*] R. Rothfelder, Dr. U. Lennert, J. Cammarata, Dr. D. J. Scott, Prof. Dr. R. Wolf

Institute of Inorganic Chemistry, University of Regensburg  
93040 Regensburg (Germany)  
E-mail: robert.wolf@ur.de

Dr. V. Streitferdt, Prof. Dr. R. M. Gschwind  
Institute of Organic Chemistry, University of Regensburg  
93040 Regensburg (Germany)  
E-mail: ruth.gschwind@ur.de

Prof. Dr. K. Zeitler  
Institute of Organic Chemistry, University of Leipzig  
04103 Leipzig (Germany)

Supporting information (SI) and the ORCID identification number(s) for the author(s) of this article can be found under:  
<https://doi.org/10.1002/anie.202110619>.

© 2021 The Authors. Angewandte Chemie International Edition published by Wiley-VCH GmbH. This is an open access article under the terms of the Creative Commons Attribution Non-Commercial NoDerivs License, which permits use and distribution in any medium, provided the original work is properly cited, the use is non-commercial and no modifications or adaptations are made.

and whose preparation involves such compounds as  $\text{Cl}_2$ ,  $\text{PCl}_3$  and molten Na (Figure 1 a).<sup>[4,5]</sup>

These deficiencies have prompted great interest in the development of alternative methodologies for the transformation of  $\text{P}_4$ ,<sup>[6]</sup> and particularly those that have the potential to furnish OPCs directly in a single reaction, without the need for laborious isolation and manipulation of potentially hazardous intermediates.<sup>[7]</sup> Unfortunately, despite extensive studies leading to numerous fundamental insights, the development of such new reactions has proven exceedingly challenging. In particular, while  $\text{P}_4$  is well known for being chemically reactive, researchers have struggled to find reactions that can selectively produce individual, useful OPCs in good yield.<sup>[8]</sup>

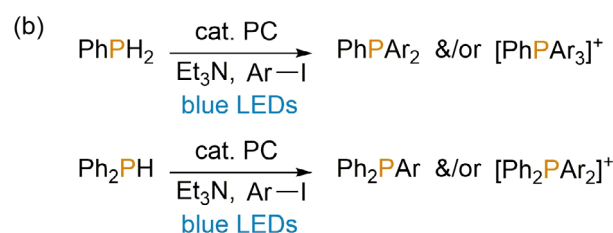
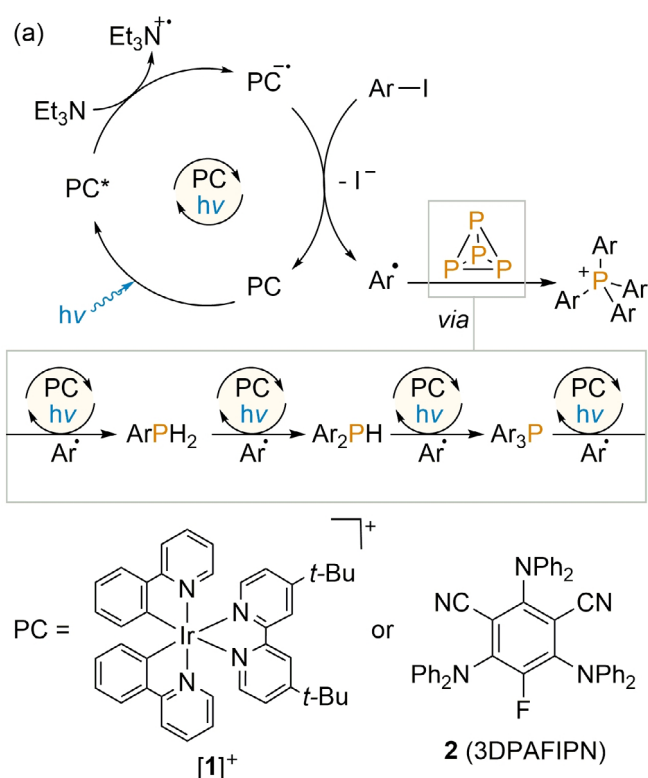
Recently, we reported a breakthrough in this area. We found that photoredox methods could be employed to successfully combine  $\text{P}_4$  with aryl iodides (ArI) to generate the corresponding  $\text{Ar}_3\text{P}$  and  $\text{Ar}_4\text{P}^+$  products under very mild conditions, often with markedly high selectivity (Figure 1 b).<sup>[9]</sup> This is the first example of such a catalytic procedure furnishing these products directly from  $\text{P}_4$ . Given the exponential growth in photoredox techniques reported over the past decade,<sup>[10]</sup> including for P–C bond formation in other contexts,<sup>[11]</sup> photoredox catalysis may also hold a much broader potential for the productive transformation of  $\text{P}_4$ .<sup>[12]</sup> Nevertheless, if this goal is to be successfully realised it is crucial to develop a deeper understanding of the mechanisms that underpin the existing photoredox reactivity of  $\text{P}_4$ .<sup>[13]</sup>

Herein we report a detailed NMR spectroscopic study on the mechanism of photoredox-catalytic  $\text{P}_4$  arylation. From the results, we have been able to draw a number of significant conclusions. These include a recognition of the importance of side reactions in determining overall product yields, a rationalisation for the differing activities of precious metal and organic photocatalysts, and the identification of a viable minor reaction pathway that involves  $\text{PH}_3$  as an early reaction intermediate. Building upon the last of these, we have been able to develop the first examples of catalytic arylation of  $\text{PH}_3$ , so providing an entirely new route to produce  $\text{Ar}_3\text{P}$  and  $\text{Ar}_4\text{P}^+$  products starting from this industrially important synthetic intermediate (Figure 1 c).

## Results and Discussion

### Previous studies and open mechanistic questions

As part of our initial report of photoredox-catalysed  $\text{P}_4$  arylation we described a series of preliminary mechanistic studies, on the basis of which we were able to propose an approximate outline mechanism for the catalytic phenylation of  $\text{P}_4$  to  $\text{Ph}_4\text{P}^+$ .<sup>[9a]</sup> This is reproduced in Scheme 1 a, and involves a fairly typical photoredox catalytic cycle for the generation of phenyl radicals ( $\text{Ph}^\cdot$  for  $\text{Ar} = \text{Ph}$ ), in which the photoredox catalyst  $[1]\text{PF}_6$  ( $1 = \text{Ir}(\text{dtbbpy})(\text{ppy})_2$ ,  $\text{dtbbpy} = 4,4'$ -di-*tert*-butyl-2,2'-bipyridine,  $\text{ppy} = 2$ -(2-pyridyl)phenyl; structure shown in Scheme 1) undergoes photoexcitation by blue light, followed by reductive quenching by  $\text{Et}_3\text{N}$  (which acts as terminal reductant in this reaction), and oxidative



**Scheme 1.** a) Outline mechanism for photocatalytic  $\text{P}_4$  arylation proposed previously; and b) recently reported photocatalytic P–H arylation of  $\text{PhPH}_2$  and  $\text{Ph}_2\text{PH}$ .

regeneration by the substrate  $\text{PhI}$ . This last redox step prompts mesolytic fragmentation of the aryl halide substrate, generating radicals  $\text{Ph}^\cdot$ . These can then add to  $\text{P}_4$  to generate in sequence  $\text{PhPH}_2$ ,  $\text{Ph}_2\text{PH}$ ,  $\text{Ph}_3\text{P}$  and  $\text{Ph}_4\text{P}^+$ , with the formation of these intermediates being observable by  $^{31}\text{P}\{^1\text{H}\}$  NMR spectroscopy. The H atoms required for formation of  $\text{PhPH}_2$  and  $\text{Ph}_2\text{PH}$  were proposed to derive from the reductant  $\text{Et}_3\text{N}$ , presumably *via* direct abstraction of H $^\cdot$  (HAT) or  $\text{H}^+$  following oxidation to  $\text{Et}_3\text{N}^{\cdot+}$ . As part of the study described herein it was possible to confirm this hypothesis through use of deuterium-labelled  $\text{Et}_3\text{N}-d_{15}$ , which led to clear deuterium incorporation into these intermediates (see Section 3.6 of the Supporting Information for further details). Subsequent loss of these H atoms was proposed to proceed by formation of  $\text{ArH}$  (observed as a byproduct by  $^1\text{H}$  and  $^2\text{H}$  NMR spectroscopy).<sup>[14]</sup>

Each of the individual arylation steps was previously confirmed to be photocatalytic. Indeed, in a recent follow-up study, we reported that the same methodology could be optimised to use  $\text{PhPH}_2$  and  $\text{Ph}_2\text{PH}$  as starting materials for

the generation of unsymmetrically substituted products (e.g.  $\text{PhPAR}_3^+$ ,  $\text{Ph}_2\text{PAR}_2^+$ ; Scheme 1b).<sup>[9b]</sup> This report also showed that the previously used precious metal catalyst  $[\mathbf{1}]\text{PF}_6$  could be replaced by the inexpensive and easily accessible organic catalyst 3DPAFIPN ( $\mathbf{2}$ ; structure shown in Scheme 1) for the arylation of both  $\text{P}_4$  and  $\text{PhPH}_2/\text{Ph}_2\text{PH}$ .<sup>[15]</sup>

Despite the superficial simplicity of the catalytic cycle shown in Scheme 1a it is clear that the overall mechanism is highly complex (we have emphasised previously that exhaustive phenylation of one equivalent of  $\text{P}_4$  requires the cleavage of six separate P-P bonds, formation of 16 new C-P bonds, and consumption of at least 16 equivalents each of  $\text{PhI}$  and  $\text{Et}_3\text{N}$ ) and that several important questions remain to be answered. From among these, at the outset of this study we identified three that are of particular significance:

1) *Is it possible to identify any other intermediate(s) formed prior to  $\text{PhPH}_2$ ?* Although  $\text{PhPH}_2$  is the first P-containing intermediate that it has been possible to observe during the phenylation of  $\text{P}_4$  thus far, it clearly cannot be the first such intermediate. Notably, by identifying  $\text{PhPH}_2$  and  $\text{Ph}_2\text{PH}$  as intermediates it has been possible to develop new functionalisation reactions of these substrates,<sup>[9b]</sup> which might also be true for any earlier intermediates.

2) *Is it possible to account for missing  $^{31}\text{P}$  intensity in these reactions?* Preliminary *in situ*  $^{31}\text{P}\{^1\text{H}\}$  NMR monitoring has shown that initial consumption of  $\text{P}_4$  is far faster than the formation of the first observable P-containing intermediate ( $\text{PhPH}_2$ ). Similarly, standard  $^{31}\text{P}\{^1\text{H}\}$  spectroscopic measurements of the final reaction mixtures suggest that formation of the target products (e.g.  $\text{Ar}_3\text{P}$ ,  $\text{Ar}_4\text{P}^+$ ) is typically very clean (no other P-containing species present, including  $\text{P}_4$ ), yet conversion to these products is consistently less than quantitative based on the initial amount of  $\text{P}_4$ .

3) *Can discrepancies in performance between catalysts  $[\mathbf{1}]\text{PF}_6$  and  $\mathbf{2}$  be explained?* Although their photoredox properties are very similar,  $[\mathbf{1}]\text{PF}_6$  has been found to give consistently higher product conversions for  $\text{P}_4$  arylation than  $\mathbf{2}$ . Conversely,  $\mathbf{2}$  has been found to provide better conversions than  $[\mathbf{1}]\text{PF}_6$  for analogous arylations starting from  $\text{PhPH}_2/\text{Ph}_2\text{PH}$ .

### Identifying new intermediates and side-products during the arylation of $\text{P}_4$

Having previously shown  $^{31}\text{P}\{^1\text{H}\}$  NMR monitoring to be a valuable tool for the investigation of the  $\text{P}_4$  arylation reaction,<sup>[9a]</sup> we reasoned that answers to our question set might be found through more detailed NMR spectroscopic analysis. For consistency with previous studies, arylation using  $\text{PhI}$  was again chosen as the simplest model system. To begin, the phenylation of  $\text{P}_4$  using organic photocatalyst  $\mathbf{2}$  was monitored over time, to provide a comparison with the analogous experiment already performed using  $[\mathbf{1}]\text{PF}_6$  as catalyst.<sup>[9a,16]</sup> As expected, a similar overall reaction profile was observed (Figure 2a), with rapid consumption of  $\text{P}_4$  followed by intermediate formation of  $\text{PhPH}_2$ ,  $\text{Ph}_2\text{PH}$  and  $\text{Ph}_3\text{P}$ , and ultimately formation of  $\text{Ph}_4\text{P}^+$  as the major reaction product. Observation of a photo-CIDNP effect in the

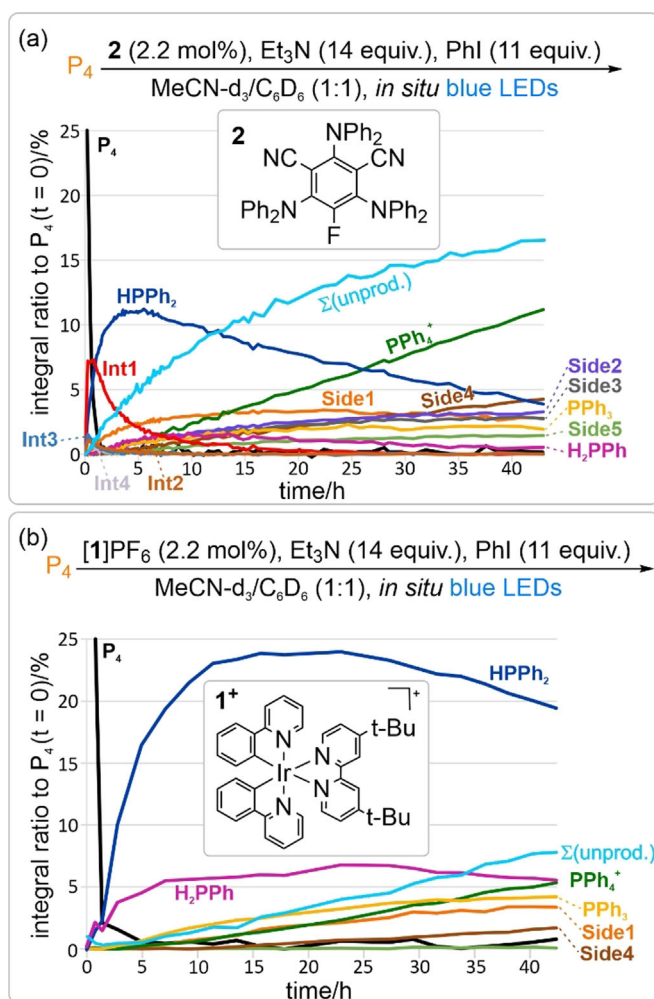


**Figure 2.** Reaction profiles showing the evolution of P atom speciation during the light-driven phenylation of  $\text{P}_4$  (0.1 mmol scale) catalysed by  $\mathbf{2}$  (a) or  $[\mathbf{1}]\text{PF}_6$  (b), as assessed by time-resolved  $^{31}\text{P}\{^1\text{H}\}$  NMR spectroscopy. Equivalents of reagent (equiv) and catalyst loadings (in mol%) are defined per P atom.  $\Sigma(\text{unprod.})$  indicates the sum of intensities for unproductive side-products Side1–Side5. For a more comprehensive display of the kinetics see Section 3.9.1 in the Supporting Information.

corresponding  $^1\text{H}$  NMR spectra was also consistent with previous observations using  $[\mathbf{1}]\text{PF}_6$  (see Section 3.8 of the Supporting Information for more details).<sup>[9a,17]</sup> Nevertheless, some qualitative differences between the two catalysts could clearly be resolved. In particular, formation of the early intermediates  $\text{PhPH}_2$  and  $\text{Ph}_2\text{PH}$  appears to peak significantly more quickly using  $\mathbf{2}$ , while the magnitude of these peaks is reduced (*c.f.* Figure 2a,b).

More dramatically, in addition to the expected intermediates  $\text{Ph}_x\text{PH}_{3-x}$  ( $x=1-3$ ),  $^{31}\text{P}\{^1\text{H}\}$  NMR monitoring clearly showed the formation of a significant number of other minor peaks during the reaction catalysed by  $\mathbf{2}$  (for representative example spectra, see Figure 3a). Some of these (designated Int1–Int4) were identified as intermediate species (either for productive or unproductive processes) based upon their concentration profile over time, while others (designated Side1–Side5) were identified as side-products and were

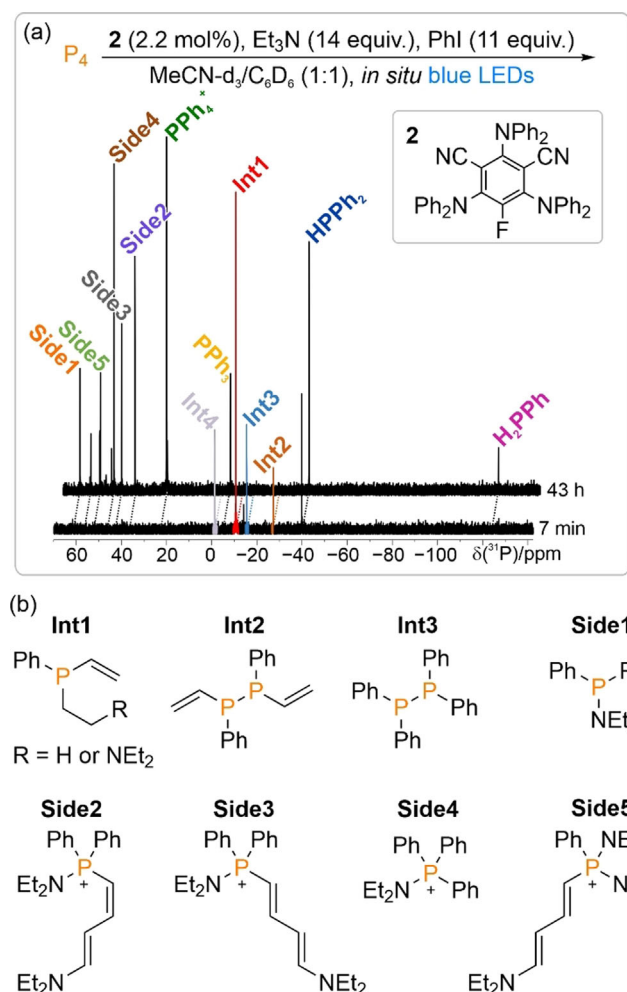


**Figure 3.** Example  $^{31}\text{P}\{^1\text{H}\}$  NMR spectra showing the formation of minor intermediates (**Int1–Int4**) and side-products (**Side1–Side5**) during the light-driven phenylation of  $\text{P}_4$  (0.1 mmol scale) catalysed by organocatalyst **2** (a); and tentatively proposed structures of these species based on *in situ* NMR data (see Sections 3.10 and 3.11 of the Supporting Information for more information) (b).

persistent until the end of the reaction (Figure 2a). The same side-products (**Side1–Side5**) could also subsequently be detected in the reaction catalysed by  $[\mathbf{1}]\text{PF}_6$ , but at appreciably lower concentrations (Figure 2b). Nevertheless, the combined intensity of these signals accounts for a significant proportion of the overall  $^{31}\text{P}$  intensity in the final reaction spectra, and it seems feasible that there may be further unresolved signals of lower intensity, which could sum to a further significant value (*vide infra*).

These observations suggest a clear explanation for less-than-quantitative target product formation highlighted above, with maximum formation of the final target products being limited by the formation of a collection of minor side products in amounts that are individually insignificant, but collectively substantial. Moreover, the fact that far greater amounts of these side-products are observed when using the organocatalyst **2** provides a rationale for the observation that **2** furnishes consistently poorer final product conversions for the arylation of  $\text{P}_4$ , despite being a more productive catalyst for

the optimised synthetic arylations of the “downstream” intermediates  $\text{PhPH}_2$  and  $\text{Ph}_2\text{PH}$  (for a discussion of catalyst performance in these latter reactions see Section 3.9.3 of the Supporting Information).

Plausible structures of the species **Int1–Int3** and **Side1–Side5** are shown in Figure 3b and are based upon detailed *in situ* NMR studies including 2D techniques and proton-coupled  $^{31}\text{P}$  spectra which are presented in the Supporting Information (Sections 3.10 and 3.11), alongside discussion of possible mechanisms of formation. As an illustrative example, the product **Side1** could be assigned based on a combination of its  $^{31}\text{P}$  chemical shift (suggestive of a  $\text{Ph}_2\text{PNR}_2$  species), long range  $^1\text{H}$ - $^{31}\text{P}$  correlation experiments (showing correlations between the  $^{31}\text{P}$  resonance and  $^1\text{H}$  signals at chemical shifts consistent with  $\text{Ph}$  and  $\text{CH}_2\text{Me}$  peaks), and comparison with literature data.

Interestingly, the majority of these species appear to be derived from non-innocent behaviour of the  $\text{Et}_3\text{N}$  terminal reductant (with the notable exception of **Int3**,  $\text{Ph}_4\text{P}_2^+$ , which was also observed in our previous investigation of the **2**-catalysed reaction of  $\text{Ph}_2\text{PH}$  with cyclohexyl iodide, and was proposed to arise through dimerization of transiently-formed radicals  $\text{Ph}_2\text{P}^\bullet$ ).<sup>[9b]</sup> Given that  $\text{Et}_3\text{N}$  is widely used as a “privileged” terminal reductant in photoredox transformations, and that  $[\mathbf{1}]\text{PF}_6$  and **2** have also been used to catalyse many other photoredox reactions, these results suggest that similar patterns of non-selective side-reactivity could be an underappreciated but highly significant limiting factor in many other photoredox transformations (indeed, related non-innocent side reactions have previously been highlighted in some other catalytic reactions).<sup>[18]</sup> In the absence of the convenient  $^{31}\text{P}$  NMR handle, these would likely be extremely challenging to detect. Minimisation of these side reactions is a clear avenue for further reaction optimisation.<sup>[19]</sup>

To try and identify further reaction intermediates—particularly those that may form in the early stages of the reaction—additional monitoring experiments were carried out on reactions performed at lower temperatures and using higher catalyst loadings. It was anticipated that transient, early intermediates might be better able to accumulate under these conditions and, indeed, several further  $^{31}\text{P}\{^1\text{H}\}$  resonances could be observed (see Figure 4a; designated **Int5–Int8**; again, these may be intermediates for either productive or unproductive processes), and plausible corresponding chemical structures assigned are depicted in Figure 4b (see also Section 3.11.1 of the Supporting Information). The proposed structures of **Int5–Int7** further emphasise the non-innocent behaviour of the  $\text{Et}_3\text{N}$  reductant.

### $\text{PH}_3$ as a substrate for photocatalytic arylation

The specific observation of  $\text{PH}_3$  as one of the above intermediate signals (**Int8**; readily assigned on the basis of its characteristic chemical shift and binomial quartet splitting in the proton-coupled  $^{31}\text{P}$  spectrum, see Figure 4a) was particularly intriguing.<sup>[3b]</sup> Although our previous mechanistic proposals (e.g. Scheme 1a) had assumed  $\text{PhPH}_2$  to be the first  $\text{P}_1$  intermediate formed, this result—combined with our previ-

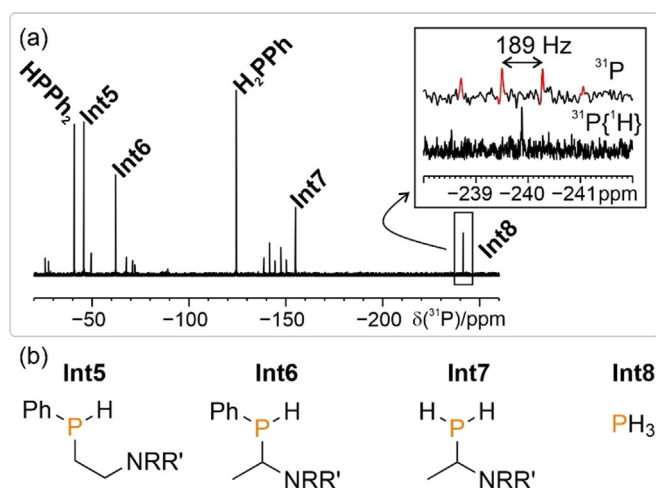


**Figure 4.** a)  $^{31}\text{P}\{^1\text{H}\}$  NMR spectrum showing the formation of further intermediates (Int5-Int8) of the light-driven phenylation of  $\text{P}_4$  (0.1 mmol scale) catalysed by [1]PF<sub>6</sub>. The spectrum was recorded in the dark after an illumination period of 30 min at 273 K (see also Section 3.11.1 of the Supporting Information). b) Proposed structures of Int5-Int8 observed during the light-driven phenylation of  $\text{P}_4$  catalysed by [1]PF<sub>6</sub> and **2** at low temperatures and high catalyst loadings.

ous observation that  $\text{PH}_3$  can be formed upon irradiation of a combination of  $\text{P}_4$ ,  $\text{Et}_3\text{N}$  and [1]PF<sub>6</sub> in the absence of ArI—suggested an alternative synthetic possibility. Specifically, it was queried whether  $\text{PH}_3$  could in fact be a key intermediate formed prior to arylation: that is, whether arylation of  $\text{P}_4$  could proceed via initial  $\text{Et}_3\text{N}$ -mediated reduction to  $\text{PH}_3$ ,<sup>[20]</sup> with arylation only subsequently occurring. Notably, such a possibility would have broad implications beyond the immediate mechanistic significance.  $\text{PH}_3$  is a major synthetic intermediate, employed industrially for the preparation of many important phosphine and phosphonium derivatives. However, these syntheses proceed exclusively through the hydrophosphination of unsaturated substrates, which limits the scope of accessible products and thereby excludes the formation of aryl-substituted derivatives ( $\text{Ar}_3\text{P}$ ,  $\text{Ar}_4\text{P}^+$ ). Indeed, efficient, direct arylation of  $\text{PH}_3$  remains a long-unmet synthetic goal that, though related, is distinct from the target of direct  $\text{P}_4$  functionalisation.<sup>[3c,4,21]</sup>

To this end, it was decided to investigate the deliberate use of  $\text{PH}_3$  as a substrate for our photo-redox-catalysed arylation methodology. For reasons of practical simplicity,  $\text{PH}_3$  was not employed directly, but rather generated *in situ* using a two-chambered apparatus, inspired by a recent report by Ball et al. (Figure 5).<sup>[22]</sup> Addition of aqueous HCl to solid  $\text{Zn}_3\text{P}_2$  in one chamber liberates gaseous  $\text{PH}_3$ , which can diffuse into the second chamber. This chamber contains the

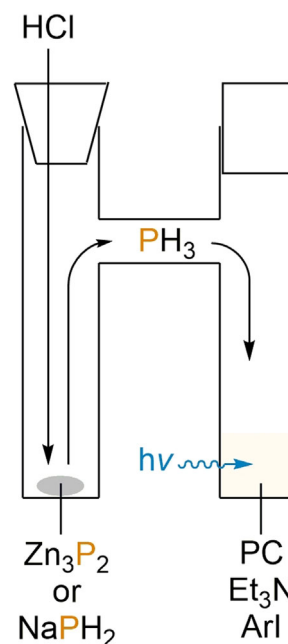


**Figure 5.** Schematic representation of the two-chambered apparatus used to investigate the photocatalytic phenylation of  $\text{PH}_3$ , generated by *in situ* acidification of suitable solid precursors.

remaining components of the photocatalytic reaction mixture and is stirred under continuous blue LED irradiation (with concomitant water cooling to maintain approximately ambient temperature).

Gratifyingly, initial experiments using catalytic [1]PF<sub>6</sub> and reaction conditions identical to those used previously in the optimised phenylation of  $\text{P}_4$  unambiguously confirmed the formation of  $\text{Ph}_4\text{P}^+$  in modest yields (Table 1, entry 1). This result clearly illustrates the feasibility of  $\text{PH}_3$  as an intermediate *en route* to arylated products and to our knowledge is the first example of the successful catalytic arylation of  $\text{PH}_3$ . Control experiments confirmed that all reaction components

**Table 1:** Photocatalytic phenylation of  $\text{PH}_3$ .

$$\text{Zn}_3\text{P}_2 \text{ or } \text{NaPH}_2 \xrightarrow{\text{HCl}} \text{PH}_3 \xrightarrow[\text{Et}_3\text{N, Ph-I, blue LEDs}]{\text{cat. PC}} \text{Ph}_4\text{P}^+$$

Entry <sup>[a]</sup>	$\text{PH}_3$ source (mmol)	PC (mol%)	$t$ [h]	Solvent	Conversion to $\text{Ph}_4\text{P}^+$ [%]
1	$\text{Zn}_3\text{P}_2$ (0.05)	[1]PF <sub>6</sub> (2)	18	MeCN/PhH (3:1)	17
2	$\text{Zn}_3\text{P}_2$ (0.15)	<b>2</b> (10)	48	MeCN/PhH (3:1)	23
3	$\text{Zn}_3\text{P}_2$ (0.15)	[1]PF <sub>6</sub> (2)	48	MeCN	30
4 <sup>[b]</sup>	$\text{Zn}_3\text{P}_2$ (0.15)	[1]PF <sub>6</sub> (2)	48	MeCN	35
5 <sup>[b]</sup>	$\text{NaPH}_2$ (0.1)	[1]PF <sub>6</sub> (2)	24	MeCN	41
6 <sup>[c]</sup>	$\text{NaPH}_2$ (0.1)	[1]PF <sub>6</sub> (2)	24	MeCN	29
7 <sup>[c,d]</sup>	$\text{NaPH}_2$ (0.1)	[1]PF <sub>6</sub> (2)	24	MeCN	68

[a] Reactions performed using a 20 mL two-chambered apparatus described in Figure 5, using 12.5 equiv HCl, 11 equiv PhI, 14.4 equiv  $\text{Et}_3\text{N}$  in 2.0 mL solvent under blue LED irradiation and  $\text{N}_2$  atmosphere. [b] A 10 mL two-chambered apparatus was used. [c] A 10 mL single-chambered apparatus was used. [d] No HCl was added. Equivalents of reagent (equiv) and catalyst loadings (in mol%) are defined per P atom.

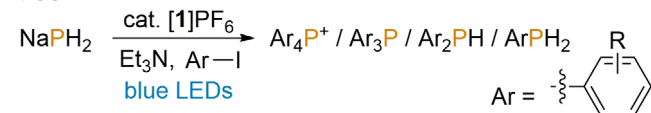
([1]PF<sub>6</sub>, Et<sub>3</sub>N, light) were necessary to achieve appreciable product formation (Table S1, SI). Catalytic formation of Ph<sub>4</sub>P<sup>+</sup> could also be achieved using organocatalyst **2** instead of [1]PF<sub>6</sub> (Table 1, entry 2), illustrating that this reactivity is not dependent on the use of a precious metal, and is mechanistically feasible for an organocatalysed reaction.

Conversion to the target Ph<sub>4</sub>P<sup>+</sup> could be significantly increased through modification of the reaction time, solvent, and concentration (Table 1, entry 3 and Table S2, SI). Although these conversions are still appreciably lower than those obtained previously when starting from P<sub>4</sub>, this may be attributable at least in part to differences in experimental setup. In particular, the need for gaseous PH<sub>3</sub> to diffuse between reaction chambers before dissolving in the reaction solution is expected to significantly impact the rate of reaction. This conclusion was supported by reactions performed using a two-chamber apparatus of reduced volume, which led to a further improvement in performance (Table 1, entry 4; for full details of the apparatus see Section 2.1 of the Supporting Information). An additional improvement was observed upon replacement of Zn<sub>3</sub>P<sub>2</sub> with NaPH<sub>2</sub>, as an alternative source of PH<sub>3</sub> upon acidification (Table 1, entry 5).<sup>[23]</sup>

To further mitigate problems associated with gas transfer of PH<sub>3</sub>, the use of a single-chambered experimental apparatus was pursued, within which it was hoped that addition of acid would trigger release of PH<sub>3</sub> directly into the photocatalytic reaction solution (for full details see Section 2.2.1 of the Supporting Information). Disappointingly, use of this apparatus in combination with NaPH<sub>2</sub>/HCl as a source of PH<sub>3</sub> did not lead to an improvement in reaction outcome, although clear catalytic formation of Ph<sub>4</sub>P<sup>+</sup> was once again observed (Table 1, entry 6). Gratifyingly, however, when this reaction was repeated in the absence of HCl significantly improved results were observed, with very good conversion to the target product achieved following slight further optimisation (Table 1, entry 7 and Table S3, SI). Thus, the conjugate base of PH<sub>3</sub> appears to be a highly effective and convenient synthetic surrogate for PH<sub>3</sub> in these reactions, allowing catalytic arylation to be performed in a practically convenient manner while achieving synthetically relevant conversion and selectivity.

Having identified an optimised set of reaction conditions for the [1]PF<sub>6</sub>-catalysed arylation of PH<sub>3</sub>, the use of other, substituted aryl iodides was investigated (Table 2). Satisfyingly, a range of other substrates ArI could be employed successfully, including examples bearing both electron-donating and electron-withdrawing groups and with varying steric bulk. These reactions yielded either phosphonium salts Ar<sub>4</sub>P<sup>+</sup> or tertiary phosphines Ar<sub>3</sub>P, with the latter being favoured for more sterically hindered substrates (notably 2-iodotoluene, which provided good conversion to the important ligand (*o*-tol)<sub>3</sub>P with good conversion and excellent selectivity; *o*-tol = 2-methylphenyl; Table 2, entry 2),<sup>[5]</sup> as well as electron-deficient substrates (such as methyl 4-iodobenzoate; Table 2, entry 7). Notably, the particularly bulky substrate MesI (Mes = 2,4,6-trimethylphenyl) failed to reach even the tertiary phosphine, instead producing the primary and secondary phosphines MesPH<sub>2</sub> and Mes<sub>2</sub>PH as the only

**Table 2:** Photoredox arylation of NaPH<sub>2</sub> (as a surrogate for PH<sub>3</sub>) catalysed by [1]PF<sub>6</sub>.



Entry <sup>[a]</sup>	R	Conversion to Ar <sub>4</sub> P <sup>+</sup> [%]	Conversion to Ar <sub>3</sub> P [%]	Conversion to Ar <sub>2</sub> PH [%]	Conversion to ArPH <sub>2</sub> [%]
1	H	77	–	–	–
2	2-Me	–	63	–	–
3	3-Me	61	6	–	–
4	4-Me	64	< 5	–	–
5	2-CO <sub>2</sub> Me	–	10	–	–
6	3-CO <sub>2</sub> Me	29	< 5	–	–
7	4-CO <sub>2</sub> Me	–	32	–	–
8	2-SMe	–	13	–	–
9	2-OMe	–	42	–	–
10	3-OMe	53	< 5	–	–
11	4-OMe	39	6	–	–
12	2-CF <sub>3</sub>	–	–	–	–
13	3-CF <sub>3</sub>	12	7	–	–
14	4-CF <sub>3</sub>	7	19	–	–
15	2,4,6-Me <sub>3</sub>	–	–	11	17
16	Ph <sub>3</sub> SnCl <sup>[b]</sup>	–	55 <sup>[c]</sup>	–	–

[a] Reactions performed using 0.1 mmol NaPH<sub>2</sub>, 2 mol% [1]PF<sub>6</sub>, 11 equiv ArI, 15 equiv Et<sub>3</sub>N in 2.0 mL MeCN under blue LED irradiation and N<sub>2</sub> atmosphere for 24 h. [b] Ph<sub>3</sub>SnCl instead of ArI. [c] (Ph<sub>3</sub>Sn)<sub>3</sub>P formed instead of Ar<sub>3</sub>P.

products detected by standard <sup>31</sup>P{<sup>1</sup>H} NMR spectroscopic measurements (Table 2, entry 15). The heteroatomic substrate Ph<sub>3</sub>SnCl could also successfully be employed, providing reasonable, selective conversion to the interesting “P<sup>3-</sup>” synthon (Ph<sub>3</sub>Sn)<sub>3</sub>P without any further reaction optimisation (Table 2, entry 16). In all cases the observed trends in reactivity and selectivity are in excellent agreement with those noted previously for the photocatalytic arylation of P<sub>4</sub>.<sup>[9]</sup>

Having established the scope of the [1]PF<sub>6</sub>-catalysed reaction, the use of the less expensive and more abundantly available, sustainable organic photoredox catalyst **2** was also investigated. Gratifyingly, after only minor further reaction optimisation (Table S4, SI), good conversions could also be achieved using this more practical, precious metal-free catalyst, under similar conditions (Table 3). In general, both catalysts achieve similar conversions, and the same trends in product selectivity are observed with respect to the substrates' steric and electronic properties. Nevertheless, in several cases an appreciably superior preference is observed for either the metallo- or organo-catalyst (for example: compare entries 2 and 9 in both Table 2 and Table 3), indicating that the choice of catalyst can be tailored to the specific target product.

### Mechanisms of photocatalytic arylation

Based on our prior studies of photocatalytic P<sub>4</sub>, PhPH<sub>2</sub> and Ph<sub>2</sub>PH arylation, as well as the studies described herein, it is possible to propose complete mechanistic courses for both

**Table 3:** Photoredox arylation of NaPH<sub>2</sub> (as a surrogate for PH<sub>3</sub>) catalysed by organocatalyst **2**.
$$\text{NaPH}_2 \xrightarrow[\text{Et}_3\text{N, Ar-I, blue LEDs}]{\text{cat. } \mathbf{2}} \text{Ar}_4\text{P}^+ / \text{Ar}_3\text{P} / \text{Ar}_2\text{PH} / \text{ArPH}_2$$

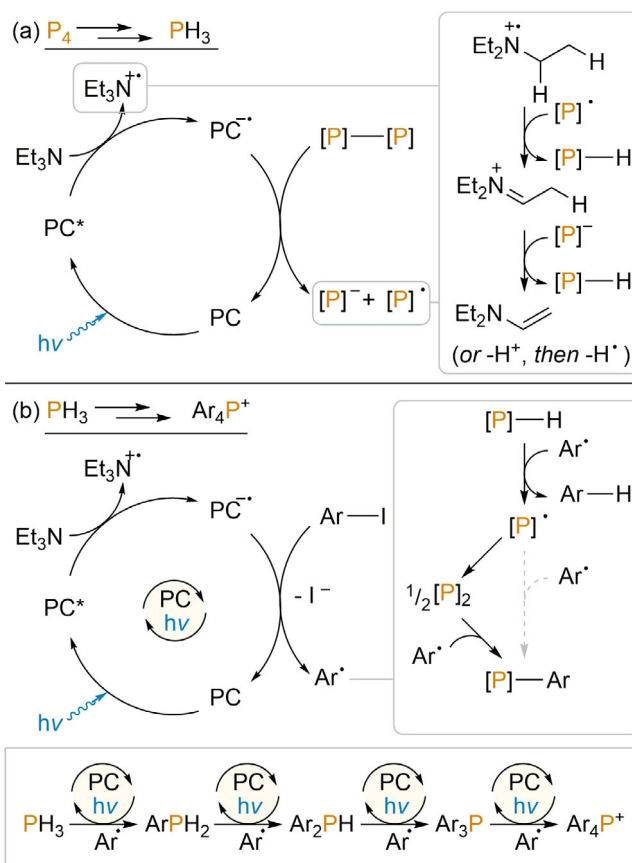
Ar =

Entry <sup>[a]</sup>	R	Conversion to Ar <sub>4</sub> P <sup>+</sup> [%]	Conversion to Ar <sub>3</sub> P [%]	Conversion to Ar <sub>2</sub> PH [%]	Conversion to ArPH <sub>2</sub> [%]
1	H	72	–	–	–
2	2-Me	–	51	–	–
3	3-Me	51	< 5	–	–
4	4-Me	56	–	–	–
5	2-CO <sub>2</sub> Me	–	7	< 5	–
6	3-CO <sub>2</sub> Me	20	< 5	–	–
7	4-CO <sub>2</sub> Me	–	9	–	–
8	2-SMe	–	29	–	–
9	2-OMe	–	52	–	–
10	3-OMe	72	7	–	–
11	4-OMe	34	14	–	–
12	2-CF <sub>3</sub>	–	–	–	–
13	3-CF <sub>3</sub>	–	6	–	–
14	4-CF <sub>3</sub>	< 5	18	–	–
15	2,4,6-Me <sub>3</sub>	–	–	7	19
16	Ph <sub>3</sub> SnCl <sup>[b]</sup>	–	41 <sup>[c]</sup>	–	–

[a] Reactions performed using 0.1 mmol NaPH<sub>2</sub>, 10 mol % **2**, 13 equiv ArI, 16 equiv Et<sub>3</sub>N in 2.0 mL MeCN under blue LED irradiation and N<sub>2</sub> atmosphere for 24 h. [b] Ph<sub>3</sub>SnCl used instead of ArI. [c] (Ph<sub>3</sub>Sn)<sub>3</sub>P formed instead of Ar<sub>3</sub>P.

the photocatalytic formation of PH<sub>3</sub> from P<sub>4</sub> and Et<sub>3</sub>N, and the photocatalytic arylation of PH<sub>3</sub> (Scheme 2). For the former, the photoexcited state of the photocatalyst PC (PC = [1]<sup>+</sup> or 2) undergoes reductive quenching by Et<sub>3</sub>N (confirmed previously by fluorescence quenching experiments) to generate Et<sub>3</sub>N<sup>•+</sup> and the reduced catalyst PC<sup>•-</sup>. Thus generated, PC<sup>•-</sup> can effect single electron reduction of one of the P-P bonds present in P<sub>4</sub> (confirmed previously by UV/Vis spectroelectrochemistry) to generate a phosphorus-centred radical and anion. Abstraction of H<sup>•</sup> and H<sup>+</sup> respectively by these species from Et<sub>3</sub>N<sup>•+</sup> (Et<sub>3</sub>N having been established as the ultimate H atom source for this chemistry; *vide supra*; for the corresponding *in situ* NMR study applying fully deuterated Et<sub>3</sub>N see Section 3.6 in the Supporting Information) then generates new P–H bonds and ultimately PH<sub>3</sub>.

Arylation of PH<sub>3</sub> is proposed to occur *via* an analogous mechanism to that already established for P–H arylation of the “downstream” intermediates PhPH<sub>2</sub> and Ph<sub>2</sub>PH. Reduction of ArI by PC<sup>•-</sup> (generated as outlined above) generates aryl radicals Ar<sup>•</sup> that can abstract H<sup>•</sup> to generate transient <sup>•</sup>PH<sub>2</sub> which can then combine with a second equivalent of Ar<sup>•</sup> to produce ArPH<sub>2</sub> (most likely *via* intermediate formation of the dimer P<sub>2</sub>H<sub>4</sub>; *c.f.* our previous observation of Ph<sub>4</sub>P<sub>2</sub> during P–H functionalisation of Ph<sub>2</sub>PH).<sup>[9b]</sup> Analogous, subsequent arylation steps then generate in turn Ar<sub>2</sub>PH and Ar<sub>3</sub>P (and, for certain Ar, Ar<sub>4</sub>P<sup>+</sup>), as established in our previous investigations. Formation of this sequence of intermediates has been further confirmed by NMR monitoring of the “single chamber” arylation of NaPH<sub>2</sub> (Figure 6).



**Scheme 2.** Complete proposed mechanisms for the photocatalytic reduction of P<sub>4</sub> to PH<sub>3</sub> in the absence of ArI (a); and the photocatalytic arylation of PH<sub>3</sub> in the presence of ArI (b). Here, [P]–[P] indicates a generic P–P bond derived from P<sub>4</sub> and [P]–H indicates a generic P–H bond derived from PH<sub>3</sub>. PC = [1]<sup>+</sup> or 2.

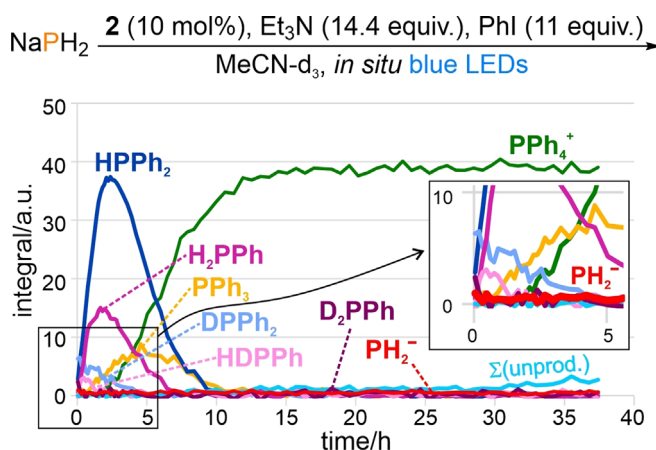
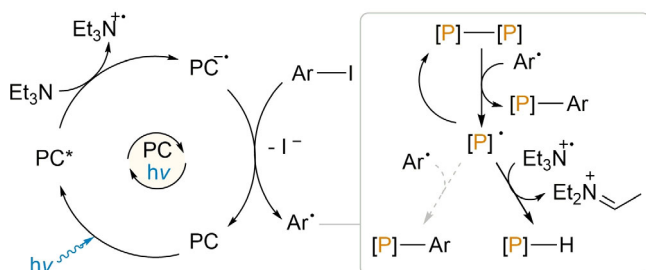


**Figure 6.** Reaction profile showing the evolution of P atom speciation during the light-driven phenylation of NaPH<sub>2</sub> (0.1 mmol scale) catalysed by organocatalyst **2**, as assessed by time-resolved <sup>31</sup>P{<sup>1</sup>H} NMR spectroscopy. Equivalents of reagent (equiv) and catalyst loadings (in mol %) are defined per P atom. Σ(unprod.) indicates the sum of intensities for unproductive side-products Side1–Side5. In the magnified region, the course of PH<sub>2</sub><sup>•-</sup> is highlighted as a thicker line to emphasize the very low amounts present throughout.

Notably, the reaction profile in Figure 6 shows that only small amounts of  $\text{NaPH}_2$  are dissolved at any specific time ( $\text{PH}_2^-$ ), and also that the sequential reaction steps leading to  $\text{PPh}_4^+$  proceed very cleanly with nearly no side product formation (*c.f.* Figure 2 for analogous, less selective reactions starting from  $\text{P}_4$ ). Based on this apparent correlation it was speculated that using lower concentrations of other monophosphorus starting materials might also provide cleaner reactions, and thus higher eventual yields. And indeed, NMR investigations of the light-driven arylation of  $\text{H}_2\text{PPh}$  (applied in different concentrations) confirmed this hypothesis by showing that the total yield of side products increases with increasing concentration of starting material, alongside a concomitant decrease in yield of the final product (for a more comprehensive discussion of side product formation during the arylation of  $\text{PhPH}_2$ , see Section 3.9.4 in the Supporting Information).

### Competing mechanisms of $\text{P}_4$ arylation

Taken together, the elementary steps outlined above (reduction of  $\text{P}_4$  to  $\text{PH}_3$  and its subsequent arylation) provide a plausible alternative mechanistic proposal for our previously reported catalytic arylation of  $\text{P}_4$ . Nevertheless, the mechanistic complexity of these reactions should again be acknowledged, and several specific observations suggest that these are unlikely to be the only kinetically viable elementary mechanistic steps. For example, it was noted in our original report that upon irradiation in the presence of  $[\mathbf{1}]\text{PF}_6$  and  $\text{Et}_3\text{N}$ ,  $\text{P}_4$  is consumed more quickly in the presence of  $\text{PhI}$  than in its absence, with the reverse being observed for consumption of  $\text{PhI}$  in the presence/absence of  $\text{P}_4$ . While the latter trend is easily explained based upon the above mechanism (since  $\text{PhI}$  must compete with  $\text{P}_4$  to react with  $\text{PC}^-$ ), the former is more difficult to account for. Moreover, attempts to quantify the  $\text{PH}_3$  formed during the photocatalytic reaction between  $\text{P}_4$  and  $\text{Et}_3\text{N}$  in the absence of  $\text{ArI}$  suggest this to be a rather inefficient process that produces  $\text{PH}_3$  in only very low yield (see Section 3.12 of the Supporting Information for full details). It is therefore likely that reaction with  $\text{Ph}^\bullet$  can provide an alternative means by which the P-P bonds of  $\text{P}_4$  are broken (Scheme 3), in line with our initial mechanistic hypothesis.<sup>[24]</sup> We thus propose that initial degradation of the  $\text{P}_4$  tetrahedron to  $\text{P}_1$  species can proceed through



**Scheme 3.** Proposed alternative initial mechanism for the photocatalytic transformation of  $\text{P}_4$  in the presence of  $\text{ArI}$ . Here,  $[\text{P}]-[\text{P}]$  indicates a generic P-P bond derived from  $\text{P}_4$ .

a combination of both pathways, to generate a mixture of  $\text{PH}_3$  and  $\text{ArPH}_2$ .<sup>[25]</sup> The relative rates, and hence importance, of these competing mechanistic routes is likely to depend strongly on the identity of the arene substrate (for example, more hindered aryl radicals may add more slowly to  $\text{P}_4$ , and so render this pathway less competitive).

### Conclusion

Detailed NMR spectroscopic studies have been used to provide a significantly deeper and more comprehensive understanding of the mechanism of our recently reported, unprecedented direct photocatalytic arylation of  $\text{P}_4$ . Despite the complexity of this elaborate transformation, it is now possible to propose a plausible and comprehensive set of elementary steps for this reaction, supported by experimental observations. In addition to these primary productive steps, it has been shown that a wide variety of competing side reactions are relevant to the overall course of the reaction, resulting in a large number of minor side products and intermediates. While these products are present in individually insignificant quantities they sum to an appreciable fraction of the overall P-containing reaction products, and their formation therefore explains the inability of these transformations to provide quantitative yields of their target products, despite full consumption of starting material and apparently clean conversion. Moreover, the use of the organophotocatalyst **2** to mediate these reactions instead of the iridium catalyst  $[\mathbf{1}]\text{PF}_6$  has been shown to significantly increase the prevalence of these side products which provides an explanation for its poorer catalytic performance in  $\text{P}_4$  arylation, despite other investigations showing it to be a superior catalyst for the closely related arylation of  $\text{PhPH}_2$  and  $\text{Ph}_2\text{PH}$ . These side products seem to be primarily derived from unexpected side reactions of the  $\text{Et}_3\text{N}$  reductant (or the aminium, iminium or enamine oxidation products thereof). Given the widespread use of  $\text{Et}_3\text{N}$  as an electron donor in photoredox chemistry, these results provide further evidence that similar side reactions may have an underappreciated limiting effect on reaction yields for many other transformations. Based on this realisation, current efforts are being made to replace  $\text{Et}_3\text{N}$  with a “better-behaved” combination of reductant and hydrogen source, to facilitate the desired transformation while minimising undesired side reactivity.

Alongside this mechanistic insight, based on the detection of  $\text{PH}_3$  as an additional intermediate, these studies have also enabled the development of an entirely new photocatalytic transformation. Specifically, the first examples of the catalytic arylation of  $\text{PH}_3$  have been developed, which allow for the unprecedented direct transformation of this key industrial  $\text{P}_1$  precursor into a sterically and electronically diverse range of valuable triarylphosphines and tetraarylphosphonium salts. Notably, this reaction does not require a precious metal catalyst, and works well using 3DPAFIPN as an inexpensive and more sustainable organic photoredox catalyst.





## Acknowledgements

We thank Gabor Balász (University of Regensburg) for a generous donation of NaPH<sub>2</sub> and Burkhard Luy (Karlsruhe Institute of Technology) for providing the broadband pulse xyBEBOP. The project was funded by the European Research Council (ERC CoG 772299), the Deutsche Forschungsgemeinschaft (DFG, German Research Foundation) – TRR 325 – 444632635, and the Alexander von Humboldt Foundation (postdoctoral fellowship for D.J.S.). Open Access funding enabled and organized by Projekt DEAL.

## Conflict of Interest

The authors declare no conflict of interest.

**Keywords:** arylation · NMR spectroscopy · phosphine · photoredox catalysis · white phosphorus

- [1] W. Gleason, *JOM* **2007**, *59*, 17–19.
- [2] D. Corbridge, *Phosphorus: An Outline of its Chemistry, Biochemistry and Technology*, Elsevier, New York, **1994**.
- [3] a) M. B. Geeson, P. Ríos, W. J. Transue, C. C. Cummins, *J. Am. Chem. Soc.* **2019**, *141*, 6375–6384; b) M. B. Geeson, C. C. Cummins, *Science* **2018**, *359*, 1383–1385; c) M. B. Geeson, C. C. Cummins, *ACS Cent. Sci.* **2020**, *6*, 848–860; d) R. W. Scholz, A. H. Roy, F. S. Brand, D. Hellums, A. E. Ulrich, *Sustainable Phosphorus Management*, Springer, Dordrecht, **2014**; e) H. Ohtake, S. Tsuneda, *Phosphorus Recovery and Recycling*, Springer, Singapore, **2019**; f) “Phosphorus”: H. Diskowski, T. Hofmann, *Ullmann’s Encyclopedia of Industrial Chemistry*, Wiley-VCH, Weinheim, **2000**.
- [4] “Phosphorus compounds, organic”: J. Svara, N. Weferling, T. Hofmann, *Ullmann’s Encyclopedia of Industrial Chemistry*, Wiley-VCH, Weinheim, **2006**.
- [5] For example: a) G. Wittig, U. Schöllkopf, *Chem. Ber.* **1954**, *87*, 1318–1330; b) G. Wittig, W. Haag, *Chem. Ber.* **1955**, *88*, 1654–1666; c) L. M. Pignolet, *Homogeneous Catalysis with Metal Phosphine Complexes*, Springer, Boston, **1983**; d) C. M. Starks, M. Halper, *Phase-Transfer Catalysis: Fundamentals, Applications, and Industrial Perspectives*, Springer, Dordrecht, **1994**; e) Z. Deng, J.-H. Lin, J.-C. Xiao, *Nat. Commun.* **2016**, *7*, 10337–10345; f) M. T. Reetz, G. Lohmer, R. Schwickardi, *Angew. Chem. Int. Ed.* **1998**, *37*, 481–483; *Angew. Chem.* **1998**, *110*, 492–495.
- [6] a) B. M. Cossairt, N. A. Piro, C. C. Cummins, *Chem. Rev.* **2010**, *110*, 4164–4177; b) M. Caporali, L. Gonsalvi, A. Rossin, M. Peruzzini, *Chem. Rev.* **2010**, *110*, 4178–4235; c) M. Scheer, G. Balász, A. Seitz, *Chem. Rev.* **2010**, *110*, 4236–4256; d) C. M. Hoidn, D. J. Scott, R. Wolf, *Chem. Eur. J.* **2021**, *27*, 1886–1902; e) L. Giusti, V. R. Landaeta, M. Vanni, J. A. Kelly, R. Wolf, M. Caporali, *Coord. Chem. Rev.* **2021**, *441*, 213927.
- [7] a) L. Xu, Y. Chi, S. Du, W.-X. Zhang, Z. Xi, *Angew. Chem. Int. Ed.* **2016**, *55*, 9187–9190; *Angew. Chem.* **2016**, *128*, 9333–9336; b) D. H. R. Barton, J. Zhu, *J. Am. Chem. Soc.* **1993**, *115*, 2071–2072; c) D. H. R. Barton, R. A. V. Embse, *Tetrahedron* **1998**, *54*, 12475–12496; d) B. M. Cossairt, C. C. Cummins, *New J. Chem.* **2010**, *34*, 1533–1536; e) S. K. Ghosh, C. C. Cummins, J. A. Gladysz, *Org. Chem. Front.* **2018**, *5*, 3421–3429; f) D. J. Scott, J. Cammarata, M. Schimpf, R. Wolf, *Nat. Chem.* **2021**, *13*, 458–464.
- [8] J. E. Borger, A. W. Ehlers, J. C. Slootweg, K. Lammertsma, *Chem. Eur. J.* **2017**, *23*, 11738–11746.
- [9] a) U. Lennert, P. B. Arockiam, V. Streitferdt, D. J. Scott, C. Rödl, R. M. Gschwind, R. Wolf, *Nat. Catal.* **2019**, *2*, 1101–1106; b) P. B. Arockiam, U. Lennert, C. Graf, R. Rothfelder, D. J. Scott, T. G. Fischer, K. Zeitler, R. Wolf, *Chem. Eur. J.* **2020**, *26*, 16374–16382.
- [10] a) N. A. Romero, D. A. Nicewicz, *Chem. Rev.* **2016**, *116*, 10075–10166; b) L. Marzo, S. K. Pagire, O. Reiser, B. König, *Angew. Chem. Int. Ed.* **2018**, *57*, 10034–10072; *Angew. Chem.* **2018**, *130*, 10188–10228; c) J. Twilton, C. Le, P. Zhang, M. H. Shaw, R. W. Evans, D. W. C. MacMillan, *Nat. Rev. Chem.* **2017**, *1*, 0052.
- [11] B.-G. Cai, J. Xuan, W.-J. Xiao, *Sci. Bull.* **2019**, *64*, 337–350.
- [12] G. Lu, J. Chen, X. Huangfu, X. Li, M. Fang, G. Tang, Y. Zhao, *Org. Chem. Front.* **2019**, *6*, 190–194.
- [13] L. Buzzetti, G. E. M. Crisenza, P. Melchiorre, *Angew. Chem. Int. Ed.* **2019**, *58*, 3730–3747; *Angew. Chem.* **2019**, *131*, 3768–3786.
- [14] Attempts to track the fate of these H atoms through use of PhPD<sub>2</sub> as a substrate proved to be complicated by rapid H/D scrambling. For full details see Section 3.7 of the Supporting Information.
- [15] E. Speckmeier, T. G. Fischer, K. Zeitler, *J. Am. Chem. Soc.* **2018**, *140*, 15353–15365.
- [16] a) C. Feldmeier, H. Bartling, E. Riedle, R. M. Gschwind, *J. Magn. Reson.* **2013**, *232*, 39–44; b) A. Seegerer, P. Nitschke, R. M. Gschwind, *Angew. Chem. Int. Ed.* **2018**, *57*, 7493–7497; *Angew. Chem.* **2018**, *130*, 7615–7619.
- [17] a) M. Goez, I. Sartorius, *J. Am. Chem. Soc.* **1993**, *115*, 11123–11133; b) M. Goez, I. Sartorius, *J. Phys. Chem. A* **2003**, *107*, 8539–8546.
- [18] For example, see L. Furst, S. Matsuura, J. M. R. Narayanam, J. W. Tucker, C. R. J. Stephenson, *Org. Lett.* **2010**, *12*, 3104–3107, and references therein.
- [19] Note however that previous screening efforts have highlighted the importance of using a reductant that can also act as a source of H atoms (presumably to facilitate formation of intermediates including PhPH<sub>2</sub> and Ph<sub>2</sub>PH), so replacement of Et<sub>3</sub>N with alternative reductants is a non-trivial task.
- [20] For reference, the standard reduction potential for aqueous reduction of P<sub>4</sub> to PH<sub>3</sub> is –0.063 V vs. SHE, which is well within the range accessible by typical photoredox catalysis. See J. R. Rumble, *CRC Handbook of Chemistry and Physics*, CRC, Boca Raton, **2021**.
- [21] “Phosphorus compounds, inorganic”: G. Bettermann, W. Krause, G. Riess, T. Hofmann, *Ullmann’s Encyclopedia of Industrial Chemistry*, Wiley-VCH, Weinheim, **2006**.
- [22] T. Barber, S. P. Argent, L. T. Ball, *ACS Catal.* **2020**, *10*, 5454–5461.
- [23] This may be due to more rapid release of PH<sub>3</sub> by NaPH<sub>2</sub>, leading to higher PH<sub>3</sub> partial pressures within the reaction apparatus.
- [24] Indeed, we have previously proposed that P-H alkylation of Ph<sub>2</sub>PH may proceed via analogous radical attack on the P-P bond of intermediately-formed P<sub>2</sub>Ph<sub>2</sub>. See also the similar mechanistic steps shown in Scheme 2b.
- [25] In principle, the use of aryl radicals Ar• to facilitate the degradation of P<sub>4</sub> could also result in formation of Ar<sub>2</sub>PH and Ar<sub>3</sub>P as direct products, although formation of these higher phosphines is likely to be less favoured on steric grounds. For Ar=Ph, direct formation of Ph<sub>3</sub>P as a major pathway is also seemingly excluded by the kinetic profiles of these reactions, which show that initial formation is very slow relative to PhPH<sub>2</sub> and Ph<sub>2</sub>PH. For Ph<sub>2</sub>PH, which forms more quickly, it is harder to confidently distinguish between formation as a P<sub>1</sub> product directly from P<sub>4</sub>, and formation by rapid arylation of PhPH<sub>2</sub>.

Manuscript received: August 7, 2021

Accepted manuscript online: September 2, 2021





Version of record online: ■ ■ ■ ■ ■ ■ ■ ■ ■ ■



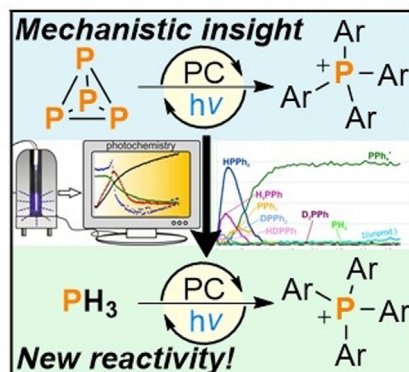
## Research Articles



## Photocatalysis

R. Rothfelder, V. Streitferdt, U. Lennert,  
J. Cammarata, D. J. Scott, K. Zeitler,  
R. M. Gschwind,\*  
R. Wolf\*    

Photocatalytic Arylation of  $P_4$  and  $PH_3$ :  
Reaction Development Through  
Mechanistic Insight



$^{31}P\{^1H\}$  NMR spectroscopic studies provide significant, new insights into the mechanism of the recently reported photocatalytic arylation of white phosphorus ( $P_4$ ). Through the first-time observation of a series of reaction intermediates, these studies have also inspired the development of the first examples of direct, catalytic arylation of  $PH_3$ , which is a key synthetic intermediate for industrial phosphorus chemistry.